Supplement of Biogeosciences, 19, 1871–1890, 2022
https://doi.org/10.5194/bg-19-1871-2022-supplement

Biogeosciences Open Access EGU

Supplement of

Low biodegradability of particulate organic carbon mobilized from thaw slumps on the Peel Plateau, NT, and possible chemosynthesis and sorption effects

Sarah Shakil et al.

Correspondence to: Sarah Shakil (shakil@ualberta.ca)

Contents:

Supplementary Methods
Supplementary Tables
Supplementary Figures

Supplementary Methods

S1 Field Processing

Stream water upstream and downstream of slump sites was collected in 10L and 4L LDPE cubitainers respectively (pre-leached with deionized water for ~24hrs). Within-slump samples were collected in acid-leached 250 – 500 mL HDPE/polyethylene bottles. In 2016, additional samples were taken at downstream sites in acid-leached 500 mL HDPE cubitainers to add as unfiltered water. All containers were triple sample rinsed.

Cubitainers containing upstream water were thoroughly shaken and a portion was decanted into a clean 4L LDPE cubitainer and stored in the dark at 4ºC until the start of the experiment. The remaining portion was geo-pump filtered through Masterflex tubing and a 1 μm pore-size Geotech filter, then filtered through pre-combusted (450°C, 5h) glass fibre filters (Whatman, GF/F, 0.7 μm) into another clean 4L LDPE cubitainer.

S2 Detailed Experimental Set-up

Prior to the start of the experiment, all sample water was brought to room temperature (~20 – 25 ºC) to prevent changing oxygen concentrations and volumes over the course of bottle filling. Experiment bottles were first filled with filtered water by drawing the appropriate filtered water sample from the cubitainer through pre-vacuumed Tygon tubing. The outlet of this tubing was placed at the bottom of the bottle to prevent air bubble formation. Due to the extremely low particulate concentrations in upstream samples, unfiltered upstream bottle treatments were also filled this way, with cubitainers gently shaken to maintain homogeneity of unfiltered water. For slump-affected treatments, unfiltered slump runoff and/or downstream water was pipetted into bottles filled with the respective filtered water. This tended to result in particulate concentrations being more dilute than *in situ* measurements. Particle suspension

was maintained prior to pipetting either by inverting bottles several times prior to pipetting or using a magnetic stir bar. Pipette tips were cut to prevent clogging. Cutting tips did not affect the volume of water drawn up, which we tested by pipetting deionized water volumes with cut tips on a weigh scale. Bottles also contained pre-sterilized and pre-combusted glass beads (MP Biomedicals, Roll & Grow^{TM} Plating Beads, MP115000550) to ensure particle suspension. In 2015, the 120 mL serum bottles were sealed with Balch blue butyl stoppers. In 2016, glass BOD bottles were used so bottles were sealed with glass stoppers wetted around the rim to ensure an air-tight seal and capped with a plastic cap to prevent any evaporation. In 2019, 120 mL serum bottles were used again and capped with grey chlorobutyl isopropene stoppers (Niemann et al., 2015).

Experiment bottles were set up in replicates of 3 – 4, with bottles processed immediately and at the end of the experiment for changes in organic carbon concentrations. Bottles processed at the end of the experiment contained oxygen sensor spots (details below) to continuously monitor oxygen concentrations during the experiment. In 2015, we intended to process bottles after 7 and 28 days, following timepoints recommended for BDOC incubations (Vonk et al., 2015) and previously used for BDOC incubations in our study region (Littlefair et al., 2017). However, due to rapid oxygen consumption at some sites, experiment bottles intended for 28 days of incubations had to be removed at 11 days to prevent anoxic conditions in the bottles that would not be reflective of stream water column conditions. Thus, for 2015 experiments we present results after 7 days of incubation. For following experiments, we aimed to conduct incubations for long enough to see a detectable change in carbon measurements, based on the declines in oxygen concentrations, while preventing experiments from going below 2 mg L^{-1} O_2. This resulted in an incubation duration of 8 days in 2016 and 27 days in 2019.

For the fractionation experiment, slump runoff collected in 2016 was stored in the dark at ~4°C until fractionation which was completed within 48 hours of collection. Briefly, 0.5 mL was poured sequentially through a 2mm 3-inch SS mesh sieve, a 63 µm sieve, and a 20 µm sieve and shaken with a cover and pan. Material that passed through the 20 µm sieve was passed through a 0.65-micron PES filter on a filter tower. Material that passed through the filter was discarded and material collected on the filter rinsed into a beaker for use in the

fractionation experiment. GF/F filtered water collected immediately downstream of slump SE was used to help rinse particles from the 0.5 mL sample through the fractionation process and make each fraction back up to an appropriate volume to compare with the unfractionated treatment, where 0.5 mL of slump runoff was diluted with filtered downstream water as necessary to approximate downstream concentrations (Table S2). There was error during this process since the sum of TSS across fractions was 61% of the TSS in the unfractionated sample (Table S2), but we still believe the relative proportion of material in each fraction is representative of the environment and provide the unfractionated control as a reference throughout.

Bottles were suspended either by placing them within a pre-drilled PVC pipe (Fig. S9) that was placed on rollers and rotated at 4 rpm (2015, 2016 bottles had to be placed sideways) or by placing them on a shaker table (2018 – 225 rpm, 2019 - ~70 rpm).

S3 Laboratory Analyses Details

S3.1 Oxygen

Oxygen concentrations were measured within air-tight bottles with SP-PSt3-PSUP-YOP-D5 oxygen sensor spots (PreSens GmbH, Regensburg, Germany, Warkentin et al., 2007). These sensor spots were attached to the inner wall of glass bottles with silicone glue. Molecular oxygen quenches the luminescence of inert metal porphyrine complex immobilized in an oxygen-permeable matrix. The photoluminescence lifetime of the luminophore within the sensor spot was measured by a fiber-optic oxygen meter (Fibox 3; PreSens GmbH) placed at the center of the spot sensor outside of the glass bottle. Excitation light (505 nm) was supplied by a glass fiber, which also transported the emitted fluorescence signal (>600 nm) back to the oxygen meter. The method does not consume any oxygen. The average of ~5 fluorescence measurements was used to determine the oxygen concentration at a timepoint. The standard deviation of these replicate measurements was always less than 0.35 mg/L. There are three factors that can interfere with oxygen measurements: (1) temperature, (2) pressure, and (3) salinity. Temperature can affect the fluorescence lifetime and the solubility of oxygen in water. Both effects are compensated for using simultaneous measurements from the temperature probe placed in an identical water experiencing the same environmental conditions as

experimental bottles. Pressure does not affect the spot sensor's measurements of mg/L of oxygen in a closed container. For our 2019 experiment, we added 1 mL of 3.6 M $ZnCl_2$ solution to sterilize half of our bottles so we corrected all bottles for a potential "salting-out-effect" oxygen (Lang and Zander, 1986) sterilized with $ZnCl_2$ in 2019 using a salinity value of 4.1 ‰.

S3.2 Organic Carbon

Filters for POC were stored frozen (1-2 months in 2015 and 2016, <2 weeks in 2019) until they were oven dried at the University of Alberta at 60 °C for 24 hours and weighed. Filters were then fumigated under heat (60 °C) for 24 hours by placing 25 mL of 12M HCl into a desiccator in an oven to remove carbonates and dolomites (Whiteside et al., 2011). Following fumigation, samples were air dried in a second desiccator and were then re-oven dried at 60 °C for 24 hours (Whiteside et al., 2011). Dried filters were packed into silver capsules, with a second layer of tin capsules to promote combustion and shipped to the GG Hatch Laboratory (now Jan Veizer Stable Isotope Laboratory, University of Ottawa) for elemental analysis on an Elementar Isotope Cube. The amount of carbon was converted to bottle POC concentrations by dividing by bottle volumes determined gravimetrically. In some cases, the entire bottle could not be filtered, and filtered volumes were determined volumetrically via a graduated cylinder. DOC concentration was determined as non-purgeable organic carbon from 3 injections with a coefficient of variation <2%, or most similar 3 of 5 injections, on a Shimadzu TOC-V analyzer at the University of Alberta. Total organic carbon concentrations were determined as the sum of DOC + POC.

S3.3 Nitrogen, Sulfur, cations, and trace metals (2019 test)

Samples for dissolved inorganic nitrogen (DIN: ammonium [NH_4^+], nitrate [NO_3^-], nitrite [NO_2^-]), SO_4^-, and trace metals were filtered through pre-combusted GF/F filters on a filter tower and stored in triple sample rinsed 15 mL centrifuge tubes. DIN tubes were pre-leached with acid and stored frozen (-20 ºC) until submission analysis at the Canadian Association of Laboratory Accreditation (CALA)-certified Biogeochemical Analytical Service Laboratory (BASL; University of Alberta, Edmonton, AB, Canada) where samples were analyzed via automated colorimetry following a modified method from US EPA 353.2. Out of each tube, concentrations of NH_4^+, NO_3^-), and NO_2^- were determined. SO_4 tubes were pre-leached with

deionized water and stored in the dark at 4 ºC until analysis at BASL where samples were analyzed via ion chromatography following a modified method from US EPA 300.1. Major ions (Na, K, Ca, Mg) and trace metals (Fe, Al, Sr, Se, Zn, Si, Ba, Mn, Ni, P, Ti, V, Rb, Li) tubes were pre-leached with acid and stored in the dark at 4 ºC. To prevent binding to the container, 4 drops of 18% trace-metal grade nitric acid was added to each tube. Samples were analyzed by inductively coupled plasma mass spectrometer (Perkin Elmer Elan 6000 Quadrupole ICP-MS) at the University of Alberta Canadian Centre for Isotope Microanalysis following Cooper et al. (2008).

S3.4 XRD (2019 test)

A subset of experimental water was filtered through a pre-combusted and pre-weighed 25 mm GF/F filter from two bottles at the beginning of the experiment to determine the mineralogy of sediments and assess whether changes in mineralogy occurred due to sterilization procedures. Filters were stored frozen (-20°C, < 2 weeks) until dried at 50-60 ºC for 24 h and weighed to record sediment weights. Mineralogy was analyzed at the University of Alberta by X-ray diffraction (XRD; Rigaku Ultimate IV). The radiation source used was a Cobalt tube at 38 kV and 38 mA. Filters were mounted on a zero-background plate and scans were conducted using Bragg-Brentano parafocusing geometry, from 5 to 90° at 0.02° steps with a scan speed of 2.00 degrees per minute (0.6 s/step). Presence of minerals was determined using JADE 9.6 software with the 2019 ICDD Database PDF 4+, and 2018-1 ICSD databases. Detection limit of the analyses is typically between 1-5%. Organic matter was not removed prior to analysis, but organic matter content of samples was below 5%. XRD analysis did not reveal any changes in mineral presence due to sterilization procedures.

S3.5 Dissolved inorganic carbon (2019 test)

Dissolved inorganic carbon samples were obtained by filtering incubation water through a 0.45 µm PES syringe filter into pre-acid-leached (10% v/v HCl, 24 hours) and pre-combusted 12 mL glass vials. Vials were sealed airtight with butyl-lined screw caps and stored in the dark at 4°C. Samples were taken in quadruplicate. In two of the replicates, we added 0.05-0.1 mL of 3.6 M $ZnCl_2$ to assess whether there was any difference in storage. Samples were measured on an Apollo SciTech DIC analyzer within 1 month of collection. For all samples, the

coefficient of variation between machine replicates was less than 0.1% and the standard deviation was less than 5 µM. For all samples without the addition of $ZnCl_2$, the coefficient of variation between tube replicates was less than 5%, and the standard deviation was less than 24 µM. We found $ZnCl_2$ has significantly lower DIC concentrations in samples and noticed precipitation of salts at the bottom of several tubes, thus we do not report DIC concentrations from DIC tubes with $ZnCl_2$ added after collection from incubation bottles.

S3.6 Optical Analyses

Dissolved organic matter composition in experimental bottles for all experiments was characterized using absorbance measurements (S3.7). In 2019, we additionally characterized DOM fluorescence and base-extractions of particulate organic matter (BEPOM)(Osburn et al., 2012) in experimental bottles. DOM samples were collected from GF/F filtrate and stored in the dark at 4°C in pre-leached HDPE bottles. Samples were analysed within 7 days of collection from experimental bottles. For BEPOM, additional bottles at the beginning and end of the experiment were filtered through pre-combusted glass fibre filters (Whatman, GF/F), and filters were stored frozen until extraction in 10 mL of 0.1 N NaOH. Further extraction details are in section S2.1 of the supplementary of Shakil et al. (2020). BEPOM was also used to characterize the organic matter pools associated with different sieve size fractions used in the 2016 experiment.

S3.7 Absorbance measurements

In 2015 and 2016, absorbance was measured at 254 nm and 750 nm on a Genesys 10 UV spectrophotomer using a 1-cm quartz cuvette. In 2019, absorbance was measured at 240-800 nm at 1nm increments in a 1-cm quartz cuvette using an integration time of 0.1 seconds (Horiba Aqualog). Absorbance values were baseline corrected either using absorbance at 750 nm (2015-16) or the mean absorbance from 700 – 800 nm (2019). Absorbance values were then converted to both decadal and Napierian absorption coefficients for calculating absorbance indices (S3.9).

S3.8 Fluorescence measurements

BEPOM samples, and 2019 DOM samples were also analysed for fluorescence (Horiba Aqualog) at excitation wavelengths of 230 – 800 nm at 5nm increments, with an integration

time of 2 seconds. Emission wavelengths spanned 117.27 – 826.70 for 2016, and 118.78 – 828.18 for 2019, both with an increment of 2.39, an integration time of 2 seconds and Medium CCD Gain. Samples were diluted when optical density was: (a) greater than 0.4 at 240 nm (Osburn et al., 2012) and/or the sum of absorbance at a pair of wavelengths was greater than 1.5 (Kothawala et al., 2013), or (b) if counts on the machine exceeded 50,000 outside the Rayleigh scatter lines (nearing the maximum number of counts the machine can record). Excitation and emission spectra were corrected using drEEM version 0.6.3 (Murphy et al., 2013). Briefly, spectra were: (a) blank corrected, using 18.2 MΩ Milli-Q water for DOM samples and neutralized 0.1 M NaOH blanks for BEPOM samples; (b) inner filter effects were corrected using matching absorbance measurements also collected at 5 nm increments; (c) fluorescence data sets were normalized to Raman Units by dividing by the Raman area of pure water integrated of a λ_{em} range 383/384 to 420/425 nm at λ_{ex} 350 nm (RU_{350}) for BEPOM and DOM samples, respectively.

S3.9 Optical Indices

For all DOM samples, we calculate $SUVA_{254}$ by normalizing the decadal absorbance at 254 nm to DOC concentrations (mg L^{-1})(Weishaar et al., 2003). $SUVA_{254}$ values were corrected for Fe concentrations estimated to be within bottles (Poulin et al., 2014) either calculated from *in situ* Fe measurements or measurements made on a subset of bottles. Using absorbance spectra, we calculated spectral slope ratios (Helms et al., 2008) for 2019 DOM samples and all BEPOM samples. From fluorescence matrices we picked the maximum fluorescence of common peaks (Coble, 2007) and normalized them to the maximum samples fluorescence to assess their relative contribution to the fluorescence landscape. We also calculated humification index for all samples, along with the biological index for DOM samples. Indices used are detailed in Table S5.

S3.10 Radiocarbon analyses

Size fractioned material retained for characterization was stored frozen (-20°C) until it was freeze dried at the University of Alberta. A portion of each freeze-dried material was subsampled using a pre-combusted stainless-steel scoopula into a new 15 mL centrifuge tube (Corning®) for radiocarbon analysis. Material subsampled for radiocarbon analysis was spread

on pre-combusted glass petri-dishes and examined under a dissecting microscope to remove any large debris or material (e.g., twigs, large rocks) that contrasted with the bulk background sediments. Subsamples of sediments were then pre-treated to remove carbonates using heated acid washes (HCl, 1M, 80ºC, 30 min; "A" treatment from Crann et al., 2017). Acid washes were repeated until effervescence stopped occurring in the samples; across all samples, two rounds of acid washes were sufficient. ^{14}C was then analyzed by Accelerator Mass Spectrometry following pellitization at the University of Ottawa (A.E. Lalonde AMS Laboratory).

S4 Sterile Experiment Details

In 2018, to test the rate of oxygen consumption on sterilized sediments, we placed 0.15 g of sterilized sediment each in 5 replicate 60 mL glass BOD bottle containing an oxygen sensor spot and glass beads to enable particle suspension, to achieve a concentration mimicking typical in-situ total suspended sediment concentrations. Bottles were filled 18.2 MΩ Milli-Q water (TOC <10ppb, sterilized in the Milli-Q system with UV-light). Bottles were sealed with a glass stopper with water placed around the rim to prevent gas exchange, along with a cap to hold the stopper in place. An additional set of 5 replicate bottles were prepared in parallel containing only Milli-Q water. All bottles and tools were sterilized with 95% ethanol which was evaporated in a fumehood. Sediment was obtained from a parallel study (Zolkos and Tank, 2020) and sterilized using dry heat in an oven set at 200°C for 24h. This sterilization procedure was validated by mixing sterilized sediment with DI water and placing 1 mL of the slurry onto a nutrient-rich agar plate at 37°C for 7 days. No colonies were observed.

In 2019, sterilization of bottles was achieved by autoclaving filtered water collected downstream of site FM3, and unfiltered water collected within slump FM3 runoff using a 30-minute sterilization procedure at 18 psi and 121°C to kill the native bacterial population. To ensure no bacterial growth if any microorganisms were introduced as the experiment was set up, we added 1 mL of ~3.6M $ZnCl_2$ solution to ensure even minimal introduction of microbes during experiment set-up would not result in rapid growth of microbes due to the absence of the original microbial community. We recognize that this removes our ability to assess whether non-stream microorganisms were introduced into the unsterilized bottles during incubation set

up. We assumed that the biotic effect of microbes introduced into unsterilized bottles during set-up would be minimal since all tools and surfaces were sterilized with 95% ethanol prior to incubation set-up and there is a microbial community present to compete with. To test sterilization, 1 mL of incubation water was pipetted onto a nutrient-rich "plate-count" agar plate, from both sterilized (see above) and unsterilized treatments. This water was removed from a bottle dedicated to BEPOM analyses where quantification of particles was not required. A sterilized glass spreader, 95% ethanol and a lighter, was then used to spread the drop around the plate evenly. The plates were then incubated under the same conditions as the incubation (20°C, in the dark). Colonies were observed to form on plates with water from unsterilized bottles, but none formed with water from sterilized bottles (Fig. S8). This test was done using bottles at the beginning and end of the experiment and still showed colony formation for unsterilized bottles but none for sterilized ones.

References

Coble, P. G.: Marine Optical Biogeochemistry: The Chemistry of Ocean Color, Chem. Rev., 107, 402–418, https://doi.org/10.1021/cr050350%2B, 2007.

Cooper, H. K., Duke, M. J. M., Simonetti, A., and Chen, G.: Trace element and Pb isotope provenance analyses of native copper in northwestern North America: results of a recent pilot study using INAA, ICP-MS, and LA-MC-ICP-MS, J. Archaeol. Sci., 35, 1732–1747, https://doi.org/10.1016/j.jas.2007.11.012, 2008.

Crann, C. A., Murseli, S., St-Jean, G., Zhao, X., Clark, I. D., and Kieser, W. E.: First Status Report on Radiocarbon Sample Preparation Techniques at the A.E. Lalonde AMS Laboratory (Ottawa, Canada), Radiocarbon, 59, 695–704, https://doi.org/10.1017/RDC.2016.55, 2017.

Helms, J. R., Stubbins, A., Ritchie, J. D., Minor, E. C., Kieber, D. J., and Mopper, K.: Absorption spectral slopes and slope ratios as indicators of molecular weight, source, and photobleaching of chromophoric dissolved organic matter, Limnol. Oceanogr., 53, 955–969, https://doi.org/10.4319/lo.2008.53.3.0955, 2008.

Klatt, J. M. and Polerecky, L.: Assessment of the stoichiometry and efficiency of CO2 fixation coupled to reduced sulfur oxidation, Front. Microbiol., 6, https://doi.org/10.3389/fmicb.2015.00484, 2015.

Kothawala, D. N., Murphy, K. R., Stedmon, C. A., Weyhenmeyer, G. A., and Tranvik, L. J.: Inner filter correction of dissolved organic matter fluorescence: Correction of inner filter effects, Limnol. Oceanogr. Methods, 11, 616–630, https://doi.org/10.4319/lom.2013.11.616, 2013.

Lang, W. and Zander, R.: Salting-out of oxygen from aqueous electrolyte solutions: prediction and measurement, Ind. Eng. Chem. Fundam., 25, 775–782, https://doi.org/10.1021/i100024a050, 1986.

Littlefair, C. A., Tank, S. E., and Kokelj, S. V.: Retrogressive thaw slumps temper dissolved organic carbon delivery to streams of the Peel Plateau, NWT, Canada, Biogeosciences, 14, 5487–5505, https://doi.org/10.5194/bg-14-5487-2017, 2017.

Murphy, K. R., Stedmon, C. A., Graeber, D., and Bro, R.: Fluorescence spectroscopy and multi-way techniques. PARAFAC, Anal. Methods, 5, 6557, https://doi.org/10.1039/c3ay41160e, 2013.

Nelson, D. C., Jørgensen, B. B., and Revsbech, N. P.: Growth Pattern and Yield of a Chemoautotrophic Beggiatoa sp. in Oxygen-Sulfide Microgradients, Appl. Environ. Microbiol., 52, 225–233, 1986.

Niemann, H., Steinle, L., Blees, J., Bussmann, I., Treude, T., Krause, S., Elvert, M., and Lehmann, M. F.: Toxic effects of lab-grade butyl rubber stoppers on aerobic methane oxidation, Limnol. Oceanogr. Methods, 13, 40–52, https://doi.org/10.1002/lom3.10005, 2015.

Osburn, C. L., Handsel, L. T., Mikan, M. P., Paerl, H. W., and Montgomery, M. T.: Fluorescence Tracking of Dissolved and Particulate Organic Matter Quality in a River-Dominated Estuary, Environ. Sci. Technol., 46, 8628–8636, https://doi.org/10.1021/es3007723, 2012.

Percak-Dennett, E., He, S., Converse, B., Konishi, H., Xu, H., Corcoran, A., Noguera, D., Chan, C., Bhattacharyya, A., Borch, T., Boyd, E., and Roden, E. E.: Microbial acceleration of aerobic pyrite oxidation at circumneutral pH, Geobiology, 15, 690–703, https://doi.org/10.1111/gbi.12241, 2017.

Poulin, B. A., Ryan, J. N., and Aiken, G. R.: Effects of Iron on Optical Properties of Dissolved Organic Matter, Environ. Sci. Technol., 48, 10098–10106, https://doi.org/10.1021/es502670r, 2014.

Shakil, S., Tank, S. E., Kokelj, S. V., Vonk, J. E., and Zolkos, S.: Particulate dominance of organic carbon mobilization from thaw slumps on the Peel Plateau, NT: Quantification and implications for stream systems and permafrost carbon release, Environ. Res. Lett., 15, 114019, https://doi.org/10.1088/1748-9326/abac36, 2020.

Vonk, J. E., Tank, S. E., Mann, P. J., Spencer, R. G. M., Treat, C. C., Striegl, R. G., Abbott, B. W., and Wickland, K. P.: Biodegradability of dissolved organic carbon in permafrost soils and aquatic systems: a meta-analysis, Biogeosciences, 12, 6915–6930, https://doi.org/10.5194/bg-12-6915-2015, 2015.

Weishaar, J. L., Aiken, G. R., Bergamaschi, B. A., Fram, M. S., Fujii, R., and Mopper, K.: Evaluation of Specific Ultraviolet Absorbance as an Indicator of the Chemical Composition and Reactivity of Dissolved Organic Carbon, Environ. Sci. Technol., 37, 4702–4708, https://doi.org/10.1021/es030360x, 2003.

Whiteside, J. H., Olsen, P. E., Eglinton, T. I., Cornet, B., McDonald, N. G., and Huber, P.: Pangean great lake paleoecology on the cusp of the end-Triassic extinction, Palaeogeogr. Palaeoclimatol. Palaeoecol., 301, 1–17, https://doi.org/10.1016/j.palaeo.2010.11.025, 2011.

Zolkos, S. and Tank, S. E.: Experimental Evidence That Permafrost Thaw History and Mineral Composition Shape Abiotic Carbon Cycling in Thermokarst-Affected Stream Networks, Front. Earth Sci., 8, https://doi.org/10.3389/feart.2020.00152, 2020.

Zolkos, S., Tank, S. E., and Kokelj, S. V.: Mineral Weathering and the Permafrost Carbon-Climate Feedback, Geophys. Res. Lett., 45, 9623–9632, https://doi.org/10.1029/2018GL078748, 2018.

Zolkos, S., Tank, S. E., Striegl, R. G., Kokelj, S. V., Kokoszka, J., Estop-Aragonés, C., and Olefeldt, D.: Thermokarst amplifies fluvial inorganic carbon cycling and export across watershed scales on the Peel Plateau, Canada, Biogeosciences, 17, 5163–5182, https://doi.org/10.5194/bg-17-5163-2020, 2020.

Supplementary Tables

Table S1. Oxygen consumption rates and absolute changes in oxygen during experiments. Note, MQ indicates 18.2 MΩ water from the Milli-Q system (described above).

Year	Treatment	Site	# days	t-half[a]		k[a]		ΔO_2 (µM)		
				mean	se	mean	se	mean	se	n[b]
2015	Filtered upstream (FU)	HA	7	49.1	5.1	0.014	0.00	-33	4	3
		HA	11	57.4	3.2	0.012	0.00	-33	1	3
		HB	7	74.8	8.9	0.01	0.00	-20	1	3
		HB	11	56.0	3.4	0.012	0.00	-34	1	3
		HD	7	35.3	4.5	0.02	0.00	-47	6	3
		HD	11	36.1	6.5	0.02	0.00	-55	8	3
	Unfiltered upstream (UU)	HA	7	35.5	3.1	0.02	0.00	-39	3	3
		HA	11	38.0	1.3	0.018	0.00	-51	2	3
		HB	7	65.7	1.6	0.011	0.00	-24	2	3
		HB	11	62.1	5.7	0.011	0.00	-38	5	3
		HD	7	8.6	0.8	0.082	0.01	-135	11	3
		HD	11	7.7	0.2	0.09	0.00	-194	6	3
	Slump in filtered upstream (SU)	HA	7	6.5	0.5	0.108	0.01	-178	10	3
		HA	11	6.2	0.8	0.116	0.01	-239	20	3
		HB	7	10.1	1.7	0.073	0.02	-121	16	3
		HB	11	12.2	0.2	0.057	0.00	-139	3	3
		HD	7	11.2	0.9	0.062	0.01	-115	10	3
		HD	11	8.0	0.6	0.088	0.01	-214	18	3
	Slump in filtered downstream (SD)	HA	7	6.4	0.5	0.109	0.01	-171	12	3
		HA	11	6.8	-	0.103	-	-226	-	1
		HB	7	10.6	0.1	0.065	0.00	-110	4	3
		HB	11	7.9	1.2	0.09	0.01	-203	33	2
		HD	7	11.7	0.4	0.059	0.00	-104	5	3
		HD	11	10.0	0.1	0.069	0.00	-178	5	3
	SU settled (SS)	HA	7	14.5	0.4	0.048	0.00	-83	5	3
		HA	11	14.8	1.1	0.047	0.00	-117	6	3
		HB	7	21.0	0.5	0.033	0.00	-57	4	3
		HB	11	21.3	0.7	0.033	0.00	-90	4	3
		HD	7	17.3	0.4	0.04	0.00	-68	3	3
		HD	11	16.5	1.0	0.042	0.00	-116	11	3
2016	Unfractionated	SE	8	6.5	0.8	0.11	0.01	-211	7	3
	2 - 0.063 mm (SN)	SE	8	23.9	2.4	0.03	0.00	-98	6	4
	0.063 - 0.020 mm (SL)	SE	8	23.8	2.0	0.03	0.00	-102	6	4
	< 0.020 mm (SMSC)	SE	8	10.1	0.3	0.069	0.00	-168	3	4

	Upstream	SE	8	63.0	13.4	0.013	0.00	-64	6	4
	Upstream filtered control	SE	8	171.8	20.6	0.004	0.00	-44	3	4
	Downstream	SE	8	13.8	2.7	0.057	0.01	-148	16	4
	Downstream filtered control	SE	8	61.6	5.1	0.012	0.00	-65	5	4
	2.79k Downstream		8	30.4	4.0	0.024	0.00	-93	4	4
	2.79k Downstream filtered control		8	109.7	32.9	0.008	0.00	-50	4	4
	MQ control		8	96.6	30.6	0.008	0.00	-44	5	2
2018	Sterile HD debris sediments	HD	7	-	-	-	-	-226	2	5
	MQ control		7	-	-	-	-	-18	4	5
	Stream	SC	27	36.4	1.5	0.02	0.00	-124	7	12
2019	Sterile control	SC	27	100.3	35.4	0.005	0.00	-15	3	12
	MQ control	NA	27	-657.9	2400.6	0	0.00	-8	5	6

[a]If k and t-half are not shown, exponential model was not an appropriate fit for data

Table S2. Comparison of 2015 TSS concentrations (mg L^{-1}) in experiment bottles at T0 vs. in situ.

Year	Site	Location	In situ		Experiment	sd	n	*Exp:InSitu*
2015	HA	Up	10.90		3.40	0.5	3	0.31
		DN[a]	2298		2100	1240	9	0.91
	HB	UP	6.87		0.62	0.5	3	0.09
		DN[a]	4330		1400	55.8	8	0.32
	HD	UP	97.1		100	0.8	3	1.03
		DN[a]	12300		1090	23.4	9	0.09
2016	SE	UP	112		104	17.3	4	0.93
		DN	46300	*unfractionated*[b]	52600	2290	4	1.14
				0.63 - 2 mm[b]	340	70.4	4	
				0.22 - 0.63 mm[b]	880	21.0	4	
				<0.22 mm[b]	30900	3740	4	
				sum of fractionated bottles	32120	3741		
				transect[c]	1190	51.6	4	0.03
		DN - 3km	20400		617	5.0	4	0.03
2018	HD	Debris Tongue			2500			
2019	SC	DN	4152		675	74.6	24	0.16

[a]SU, SS, and SD treatments were mimicking downstream conditions.

[b]used within-slump particles and downstream filtrate (fractionation experiment)

[c]used donwstream particles and filtrate (for transect experiment)

note: low Exp:InSitu ratios for upstream locations with low TSS values may be detection limit issues of TSS

In Situ TSS measurements at many upstream sites required filtering of upwards of 1-2 L of water. Experimental bottle volumes were 60-120 mL.

Table S3. Presence of minerals, as detected by XRD analysis, of sediments in bottles at the beginning of the experiment.

	Treatment		Stream		Sterile
	Rep	A	B	A	B
Calcite	$Ca(CO_3)$	Y	Y	Y	Y
Pyrite	FeS_2	Y	Y	Y	Y
Gypsum	$CaSO_4 \cdot 2H_2O$	N	N	N	N
Quartz	SiO_2	Y	Y	Y	Y
Muscovite	$KAl_2(Si,Al)_4O_{10}(OH_2)$	Y	Y	Y	Y
Albite	$NaAlSi_3O_8$	Y	Y	Y	Y
Clinochlore	$(Mg,Fe,Al)_6(Si,Al)_4O_{10}(OH)_8$	Y	Y	Y	Y
Kaolonite	$Al_2Si_2O_5(OH)_4$	Y	Y	Y	N
Microcline	$K(AlSi_3O_8)$	Y	Y	Y	Y

Table S4. Estimated initial ammonium concentrations associated with experiments where gains in organic carbon were significantly greater than zero.

Year	Treatment	Site	# days	n	ΔTOC (μM)	ΔTOC CI error	Oxygen consumed (μM)	CI error	Estimated initial NH_4^+ (μM)
2015	Filtered (F)	HB	11	3	130	67	34	4	0.53
	Unfiltered Upstream (U)	HD	11	3	150	28	194	24	3.3
	Slump in filtered upstream (SU)	HA	7	3	269	250	178	43	1.4
		HB	11	3	335	296	140	14	0.65
	Slump in filtered downstream (SD)	HA	7	3	337	285	171	50	7.9
		HA[a]	11	1	418	-	226	-	7.9
	SU settled (SS)	HB	7	3	164	164	57	16	0.65
2016 - Fractionation	<0.020 mm	SE	8	4	601	459	168	8	not collected
2016 - Transect	Upstream	SE	8	4	75	60	64	20	not collected
	Upstream filtered control	SE	8	4	37	36	44	9	
	~3k Downstream		8	4	60	50	93	13	not collected
	Milli-Q water control		8	3	83	71	44	59	0.0

[a] only 1 sample because other bottle replicates went before 2 mg L^{-1}

Table S5. Description of optical indices used.

	Index or Component	Calculation	Reference	Description / Purpose
Abs-based	S_R	$S_{275-295}$ / $S_{350-400}$	Helms et al. (2008)	Shown to be negatively correlated to DOM molecular weight and to generally decrease on irradiation
	$SUVA_{254}$ (Fe-corrected)	Decadal absorbance, corrected for Fe absorbance, normalized to path length and DOC concentrations	Weishaar et al. (2003), Poulin et al. (2014)	Greater values indicate greater aromaticity of the DOM pool, suggesting lower biolability
Fluor. Based	Humification Index (HIX)	$\sum I_{em\ 435-480}$ / ($\sum I_{em\ 300-345}$ + $\sum I_{em\ 435-480}$) at ex. 254	Ohno et al. (2002)	Ranges from 0 to 1, with increasing values associated with a "red-shift" or shift to longer wavelengths, potentially due to lower molecular ratios of hydrogen to carbon. May indicate relative abundance of compounds generated through polycondensation reactions. This could indicate material further in the progression in organic matter decay and greater relative abundance of compounds more resistant to breakdown (refractory).
	Biological Index (BIX)	$I_{em\ 380}$ / $I_{em\ 430}$ at ex. 310	Huguet et al. (2009)	Modified from the original freshness index (see Freshness Index) to account for broadening of 'humic' region by presence of α peak. In this study, freshness index and biological index are perfectly correlated.
	<u>Common Coble peaks normalized to maximum Fluorescence</u>			

B	Ex: 275, Em: 305	Coble et al. 2007	tyrosine-like, protein-like
T	Ex: 275, Em: 340	Coble et al. 2007	tryptophan-like, protein-like
A	Ex: 260, Em: 400-460	Coble et al. 2007	UVC-humic-like
C	Ex: 320-360, Em: 420-460	Coble et al. 2007	UVA humic-like
M	Ex: 290-310, Em: 370-410	Coble et al. 2007	UVA humic-like
Components based on previous PARAFAC analyses normalized to maximum Fluorescence			
C1		Shakil et al. 2020	degraded terrestrial-like; similar to Coble peak A
C3		Shakil et al. 2020	fresher terrestrial-like (relative to C1), similar to Coble peak C
C5		Shakil et al. 2020	protein-like

Table S6. Final list of optical indices input to the PCA analyses, and their relationship to indices that were removed due to strong correlation. See Table S5 for abbreviations.

Group	Optical Indices	Other Indices with Pearson correlation >0.9
2016 Experiment Size Fractions	S_R	Peaks B, M
	HIX	none
	Peak A	none
	Peak C	$a_{Tot.\ 250450}$
2019 Experimental DOM samples	$SUVA_{254}$	HIX, A
	S_R	none
	Peak C	Peak A
	Peak M	Peak T
	BIX	Peaks B, T
2019 Experimental BEPOM Samples	S_R	none
	HIX	Peak C, Component C3
	Peak M	none
	C1	Peaks A, B, T, Component C5
	C2	Peaks A, B, C5

Supplementary Figures

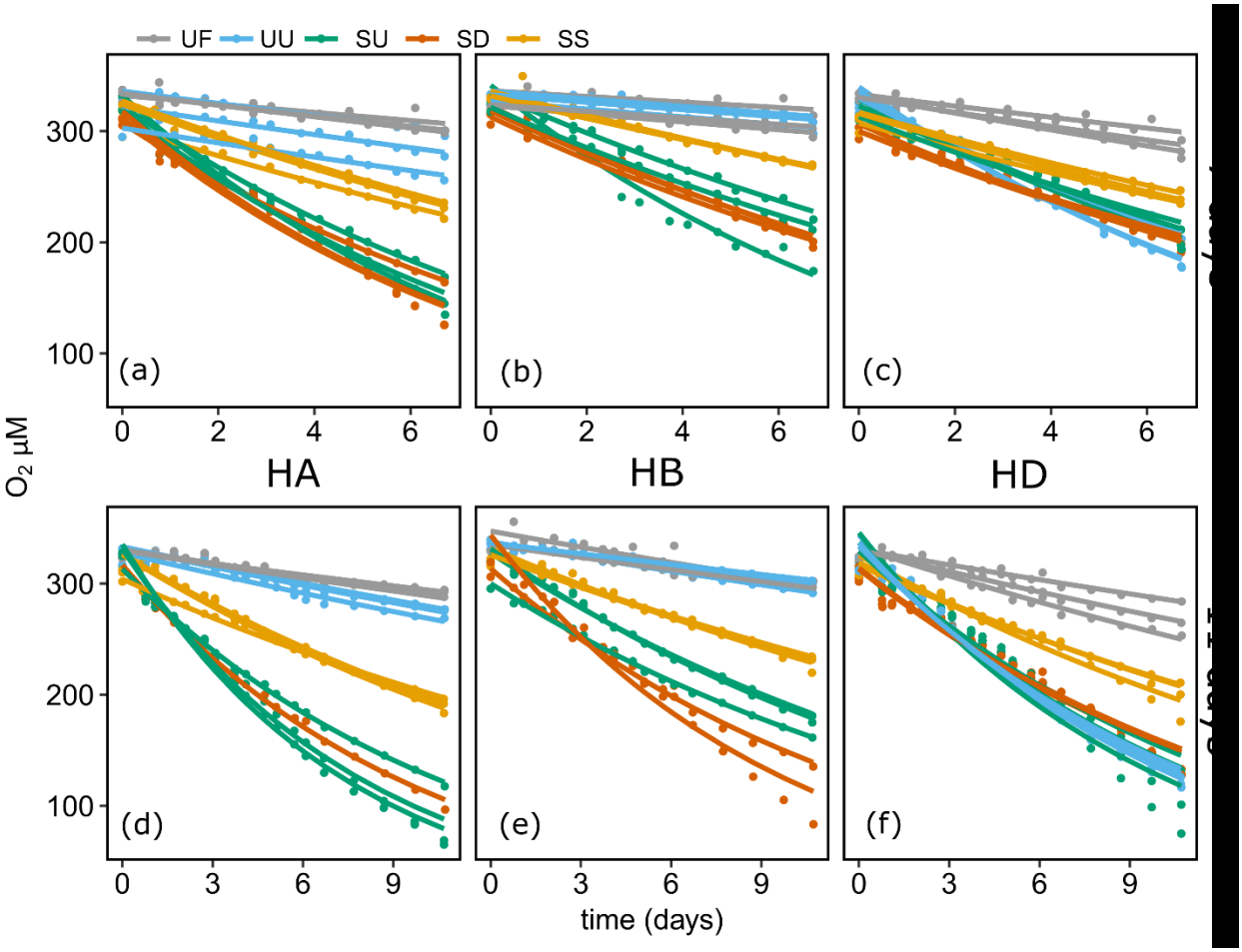

Figure S1. 2015 experiment oxygen concentrations (µM) for bottles incubated for 7 days (a-c) and 11 days (d-f). Dots show measured concentrations and lines show modelled measurements based on first order exponential decay. HA, HB, and HD differentiate slump sites. Codes: filtered (UF) and unfiltered (UU) upstream, slump material in upstream (SU) and downstream (SD) filtrate, and SU settled out (SS).

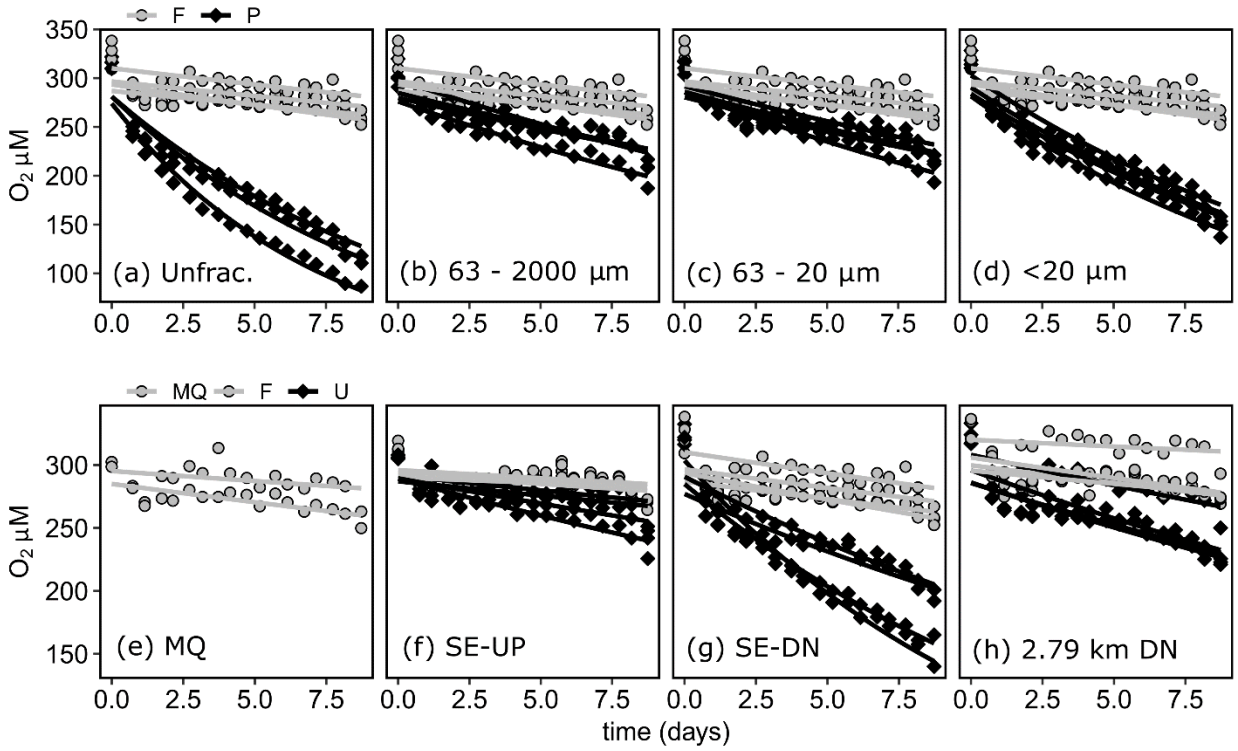

Figure S2. 2016 experiment oxygen concentrations for fractionation experiment (a-d) and transect validation experiment (e-h). Codes in a-d differentiate filtered controls (F) and particle containing bottles (P) and codes for e-h differentiate Milli-Q control (MQ) filtered controls (F) and unfiltered treatments (U). Note that F in a-d and g are from the same samples, but repeatedly shown for easy comparison. Dots show measured concentrations and lines show modelled concentrations based on first order exponential decay.

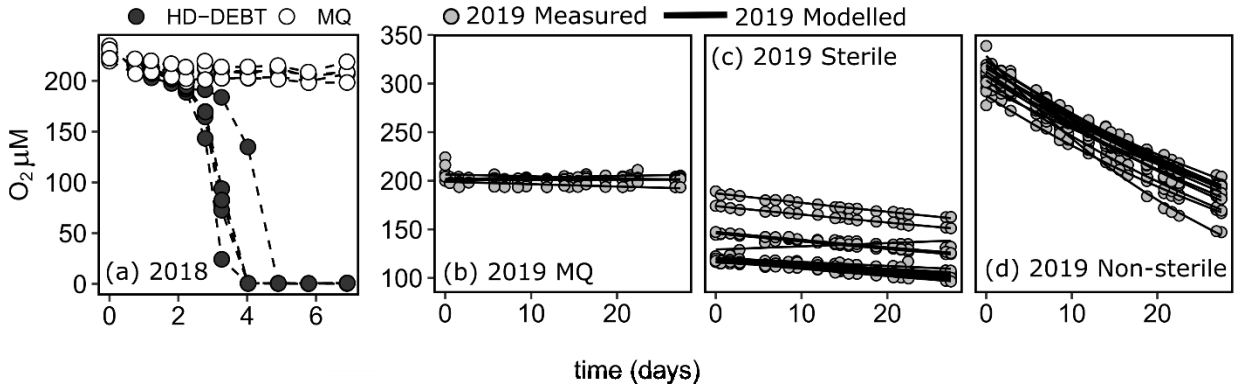

Figure S3. 2018 (a) and 2019 (b-d) oxygen concentrations (µM). Dots show measured concentrations. Dashed lines in (a) are just used to connect repeat measurements from the same bottle while solid lines in b-d show modelled measurements based on first order exponential decay. HB-DEBT = HD debris sediments, MQ=Milli-Q water.

Figure S4. Damming of upstream flow by HD debris and encroachment of slump material into the upstream site following the formation of a debris dam by slump outflow.

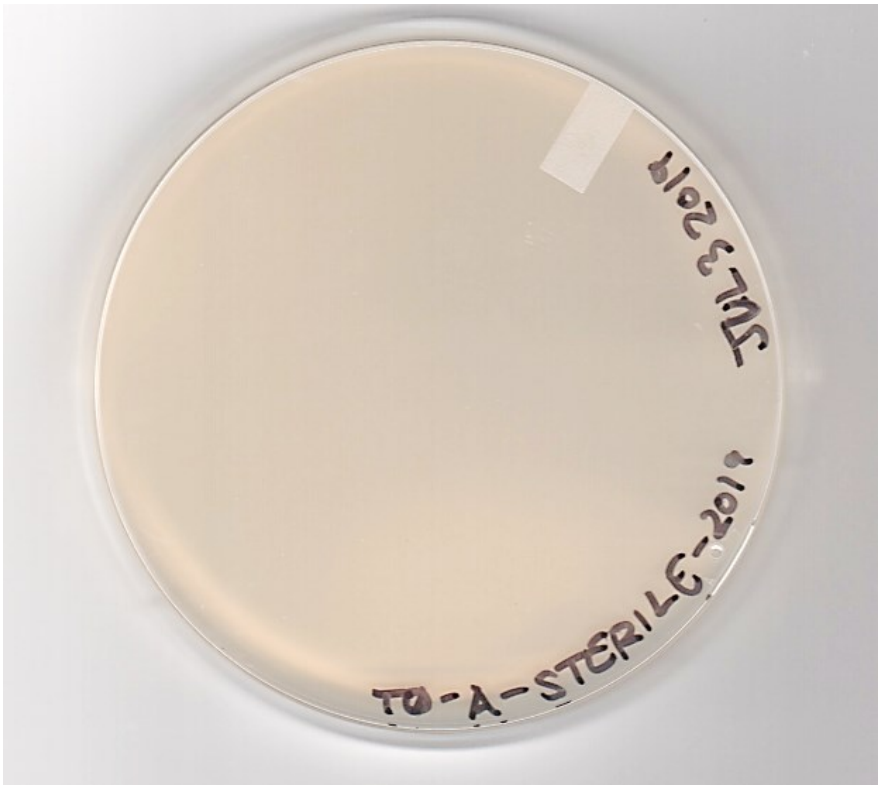
TØ-A-STERILE-2019
JUL 3 2019

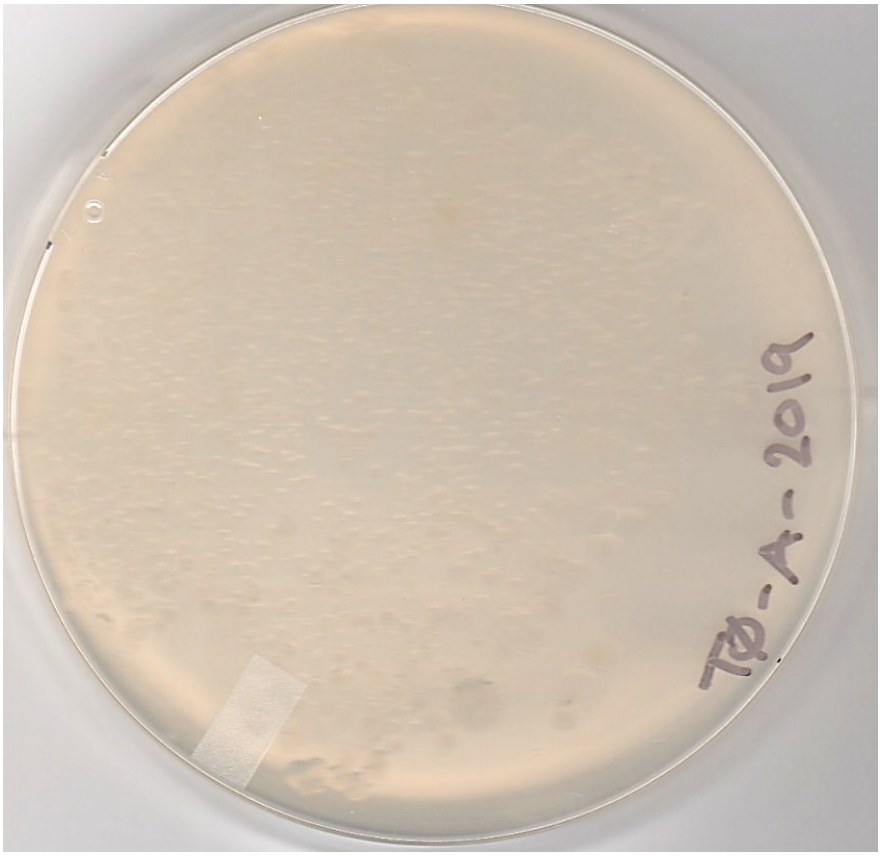
TØ-A-2019

Figure S5. Microbial count of sterilized (top) and unsterilized (bottom) bottles from the 2019 experiments. Note on bottom, light coloured bumps represent microbial colonies.

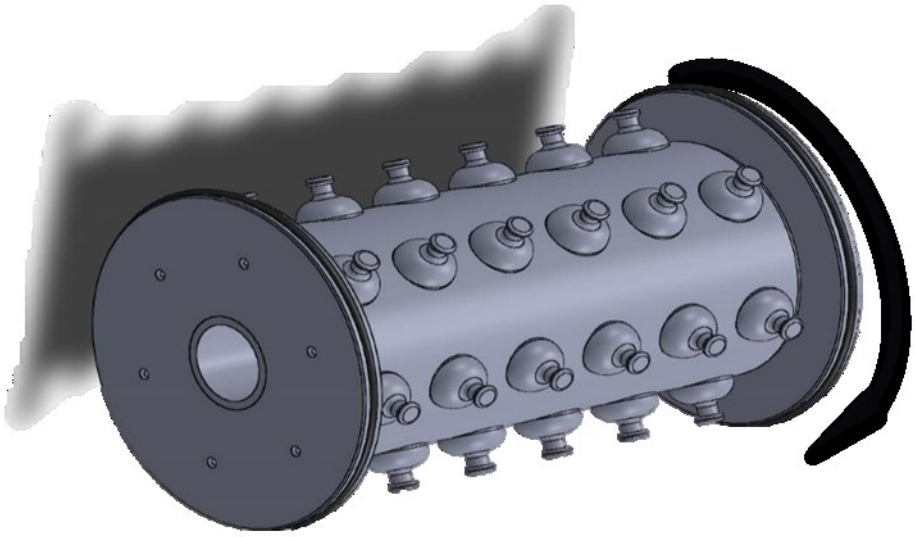

Figure S6. Schematic diagram of rotator used for particle suspension in 2015.